Electronic Supplementary Material (ESI) for Environmental Science: Nano.

Supporting Information

Interactions between Polystyrene Nanoparticles and Supported Lipid Bilayers:

Impact of Charge and Hydrophobicity Modification by Specific Anions

Zehui Xia[a], April Woods[b], Amanda Quirk[b], Ian J. Burgess[b], Boris L. T. Lau[a]

[a]*Department of Civil & Environmental Engineering, University of Massachusetts Amherst, 130 Natural Resources Road, Amherst, MA 01003, USA*

[b]*Department of Chemistry, University of Saskatchewan, 110 Science Place, Saskatoon, SK S7N5C9, Canada*

Correspondence: Boris L. T. Lau

E-mail: borislau@umass.edu

Preparation of DOPC lipid vesicles

For the preparation of DOPC vesicles, 0.1 ml of 25 g/L DOPC (Figure S1) in chloroform was dried under a flow of nitrogen until a thin and even film was formed at the bottom and on the wall of the test tube, after which the nitrogen stream was continued for another 15 minutes to ensure the removal of remaining solvent. The tube coated with the DOPC film was left in a desiccator overnight before use. The dried lipids were then resuspended and hydrated in 2.5 mL of 50 mM PBS and vortexed periodically for about 1 minute. To obtain small unilamellar vesicles, the mixture was sonicated in an ultrasonic water bath (FS 30, Fisher Scientific) for approximately 1.5 hours at room temperature until it became clear. The suspension was then filtered through a 0.2 μm membrane to remove large vesicles. Same buffer solution was applied to dilute the concentration to 0.1 g/L, after which the vesicle suspension was stored at 4 ºC and ready to use. All lipid vesicle solutions were used within 1 week of preparation.

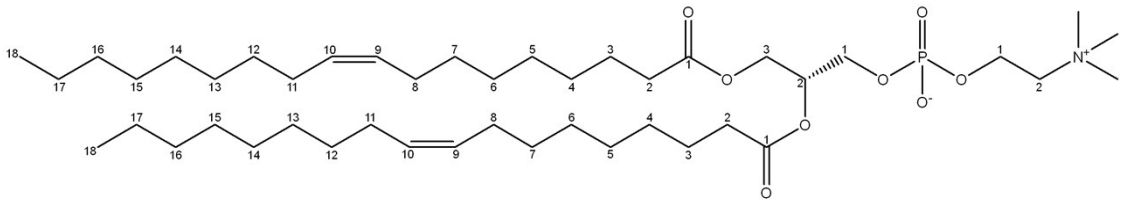

Figure S1. Molecular structure of DOPC.

Formation of SLB on silica sensors monitored by QCM-D

Vesicle fusion on silica sensor surface follows the procedures described by Cho et al.[1] After the baseline of buffer was stabilized, DOPC vesicles were introduced into the QCM-D module at a flow rate of 0.1 mL/min. The deposition of lipid vesicles onto the sensor caused a negative Δf and positive ΔD (Figure S2).

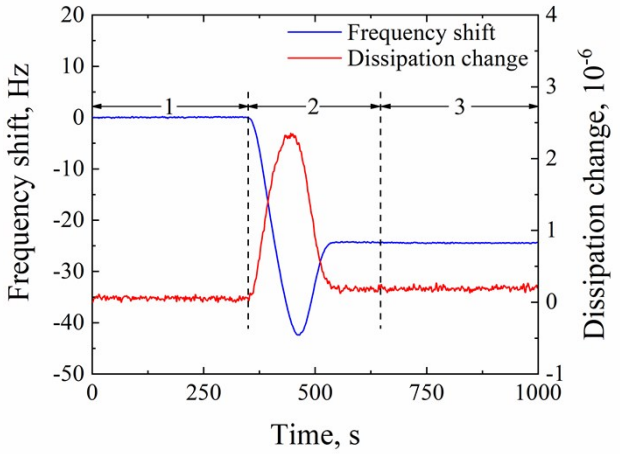

Figure S2. Frequency shifts (blue) and dissipation changes (red) monitored by QCM-D during the formation of SLB at 50 mM PBS, pH 7.5. A typical experiment consists of stages illustrated in the figure: (1) buffer solution only; (2) introduction of NPs; and (3) buffer solution only.

When a critical surface coverage point was reached, SLB was formed after the release of water encapsulated in the vesicles, leading to a positive Δf and negative ΔD. Buffer was then injected to rinse and stabilize the bilayer, after which Δf and ΔD were approximately -24 Hz and 0.2 x10^{-6} respectively. These values are consistent with previous studies.[1-3]

Flame annealing of the gold film

In SEIRAS, the as-formed gold film was annealed with a small flamed butane torch for five 15-second intervals, 30 seconds wait time between each interval, and finally cooled for 60 minutes. The film was rinsed under a stream of milli-Q water before and after annealing and electrochemically cleaned in 50 mM NaF. The flame annealing was found to improve adhesion of the gold layer to the silicon hemisphere and resulted in a surface better suited for vesicle fusion of a supported lipid bilayer. Infrared light passing through the prism undergoes total internal reflection at the prism/solution interface and the resulting evanescent wave couples with surface plasmon polariton modes of the metal resulting in large electric fields at the interface. The magnitude of the electric field decays rapidly from the surface rendering the IR absorption enhancement limited to molecules at or very near the metal surface.

Solvent-assisted lipid bilayer (SALB) formation monitored by SEIRAS

A challenge in using SEIRAS for studying SLB is identifying a suitable means to assemble the bilayer on the metallized surface. Glass surfaces are highly hydrophilic due their negative surface charges and allow lipid vesicles to rupture, fuse and evenly spread on thin layers of water that cushion the bilayer from the solid support. Conversely, clean gold is quite hydrophobic and excludes the thin water layer that helps effect facile vesicle spreading. Fusion of cholesterol containing DMPC vesicles onto gold surfaces has been extensively reported by Lipkowski and co-workers[4, 5] but the relatively high roughness of SEIRAS substrates impedes vesicle rupture and spreading unless the surface is smoothened by flame-annealing which can greatly attenuate the enhancement effect. Previous strategies for performing SEIRAS on SLB used either direct vesicle fusion[6] or a hybrid bilayer approach whereby the proximal layer is actually a long-chained SAM of an alkyl thiol and the distal layer is formed by vesicle fusion.[7]

Solvent-assisted lipid bilayer (SALB) formation is an alternative method to form continuous and uniform SLBs on gold surfaces.[8, 9] SALB involves the slow, continuous flow of aqueous buffer into the organic phase containing dissolved lipid in which the solid substrate of interest is immersed. We adapted the procedure outlined by Tabaei et al[8] to our SEIRAS

spectroelectrochemical cell. Briefly, a spectroelectrochemical cell containing the gold film on which the lipid bilayer is to be supported is filled with isopropanol containing 0.5 mg/mL DOPC. Then, 50 mM PBS is introduced at a flow rate of 50 µL/min over several hours until bilayer fusion is complete. Here we followed the DOPC deposition as a function of time by plotting the peak absorbance intensity at ca. 2928 cm^{-1} during the solvent exchange (Figure S3a). All SEIRA spectra were measured with a Bruker (Vertex 70) spectrometer equipped with a VeeMAX II ATR accessory (Pike Technologies). The spectral resolution was 4 cm^{-1} and 1024 interferograms were co-added for each spectrum. The sample chamber of the spectrometer was purged throughout the experiment using CO_2 and H_2O–free air. The results of Figure S3a indicate that although lipid deposition by the SALB procedure is slow, a clear saturation behavior can be observed after ~ 4 hours of solvent exchange.

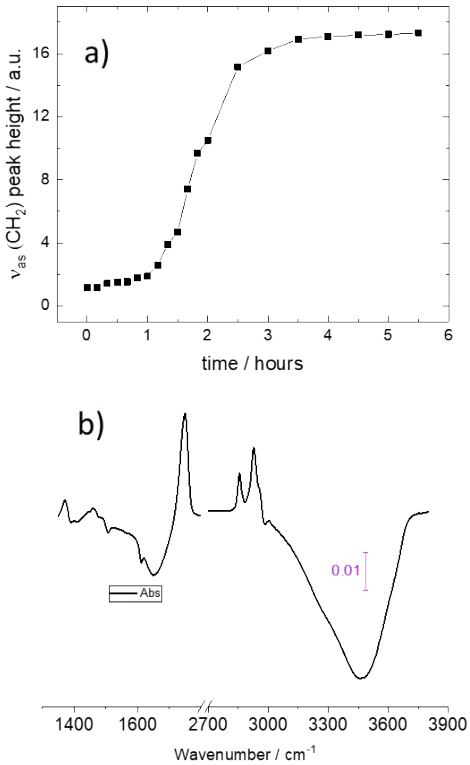

Figure S3. a) Peak height as the function of time during the formation of SALB. b) SEIRAS spectrum during vesicle fusion of DOPC on gold film.

Furthermore, as shown by the resulting SEIRA spectrum in Figure S3b, the SALB method provides intense IR absorption bands in the C-H stretch region (~2800 – 3050 cm^{-1}), the C=O

stretch region (~ 1750 cm^{-1}) and the C-H bending region (~1360-1500 cm^{-1}). The weak peak observed at 3005 cm^{-1} can be assigned to the C-H stretch in the unsaturated oleoyl group. The positive-going absorption peaks at 2928 cm^{-1} and 2855 cm^{-1} are assigned to the asymmetric and symmetric stretching modes of the methylene (CH_2) units of the lipid tail groups. The frequency of the former is highly sensitive to the conformational order in the aliphatic chain and frequencies lower than 2920 cm^{-1} are associated with highly ordered (all-trans) C-H chains. The higher frequency CH_2 asymmetric stretch observed in Figure S3b is typical for DOPC in its liquid state[10, 11] and consistent with the reported gel-liquid phase transition temperature of -22°C.[12] The position of the C=O stretch mode at 1748 cm^{-1} is considerably higher in frequency than the values reported for highly hydrated ester groups in DOPC directly adsorbed to weakly charged gold surfaces. Zawisza et al[11] have shown that displacement of DOPC bilayers from the gold surface by thin layers of water leads to dehydrated ester groups and similar peak positions for the C=O stretch to those reported above. The large, negative bands appearing in the spectrum arise from the displacement of water and isopropanol from the surface upon formation of the DOPC SLB. Other distinctive vibrational modes such as the P-O stretch of the headgroup are at frequencies below the transparency cutoff of the Si prism. After SALB formation, increasing concentrations of NP suspension up to 0.1 g/L were added to the reaction cell, followed by introduction of increasing electrolyte solutions to a final 150 mM ionic strength. A SEIRA spectrum after DOPC bilayer formation was used as the reference. Downward peaks indicate a decrease in absorption for a given vibration mode, due to either a less mass density or a diminishing alignment of the transition dipole perpendicular to the substrate surface. Upward peaks demonstrate the increase of the vibration either in density or alignment.

Effect of ionic strength on NP-SLB interactions

The QCM-D experiment was repeated at a lower ionic strength of 10 mM for both types of NPs to further evaluate the contribution of electrostatic forces. In the case of PS-COOH, the ionic strength significantly affected the deposition of NPs on SLB. There was a relatively minor Δf of approximately -1.7 Hz and ΔD of 0.5 × 10^{-6} (Figures S4a and S4b) at 10mM NaF, in contrast to a Δf of -360 Hz and a ΔD of 76 × 10^{-6} at 150 mM ionic strength (Figure 1a and 1b).

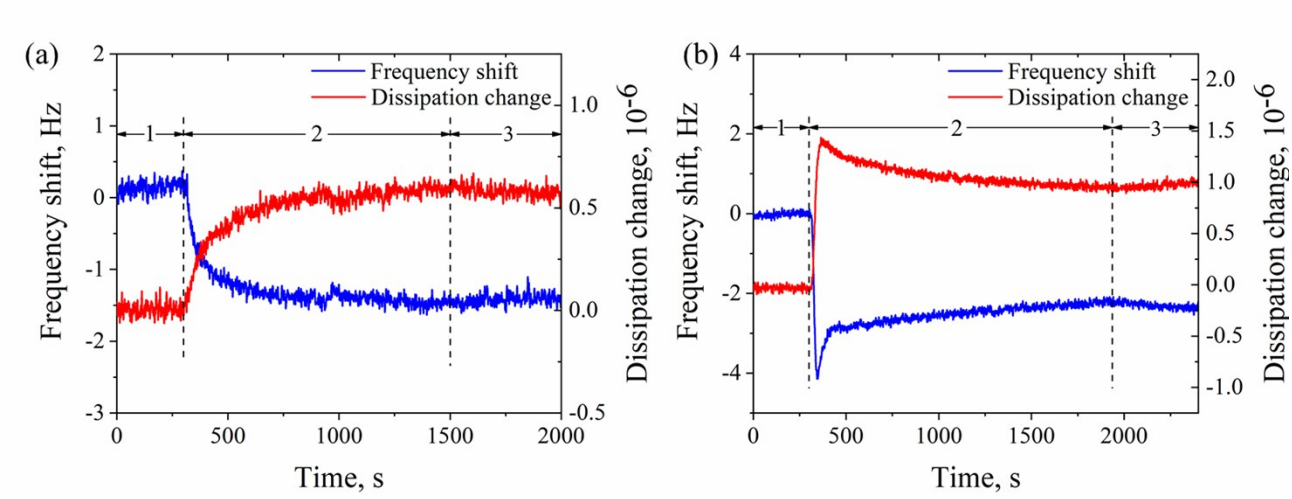

Figure S4. Frequency shifts (blue) and dissipation changes (red) monitored by QCM-D during the deposition of PS-COOH (a) and PS-NH_2 (b) onto SLB at 10 mM NaF, pH 7.5. A typical experiment consists of stages illustrated in the figure: (1) buffer solution only; (2) introduction of NPs; and (3) buffer solution only.

SEIRAS spectrum at 10mM also confirmed the minor perturbation of SLB by PS-COOH, which largely consisted of the observation of a positive absorption band at C=O region (~ 1752 cm^{-1}, Figure S5a) and very small negative absorption changes in OH stretch region (~ 3450 cm^{-1}, Figure S5a). The positive one may rise from either an orientation change of lipid head groups of the DOPC molecules or from the carboxylic acid groups of PS-COOH that displaced the interfacial water. In either case, the PS-COOH-SLB interaction was minimal at 10 mM NaF and there was no evidence of significant disruption of the DOPC bilayers. SEIRAS spectrum at 150mM is shown in Figure S6 for comparison purposes.

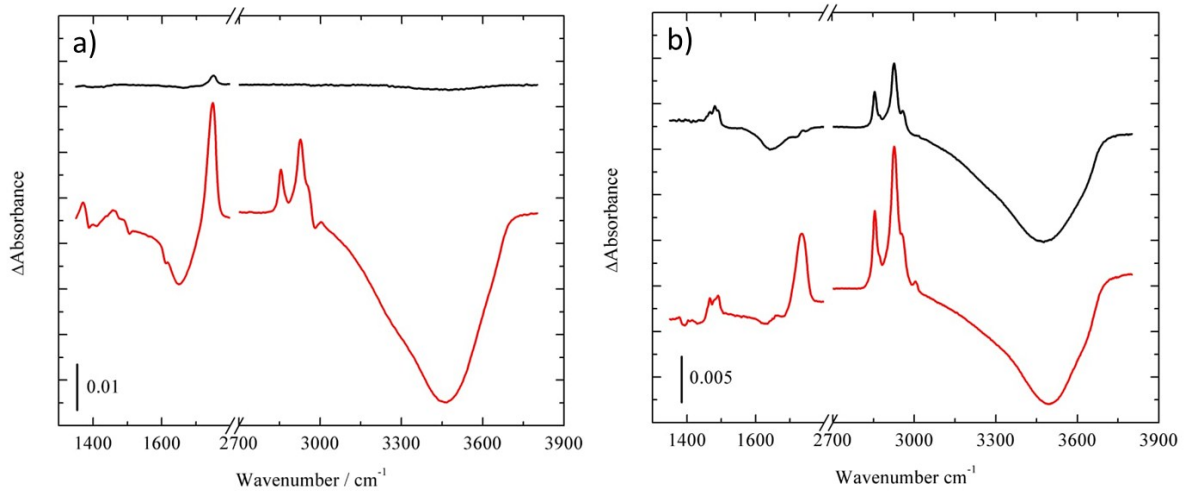

Figure S5. SEIRAS spectra recording the deposition of PS-COOH (a) and PS-NH_2 (b) onto SLB at 10 mM NaF, pH 7.5. The spectra are presented as the change in absorbance referenced to the interface before adding NPs and after the formation of DOPC bilayer (black lines). Alternatively, the spectra are shown using the single beam spectrum prior to the formation of the bilayer as the reference spectrum (red lines).

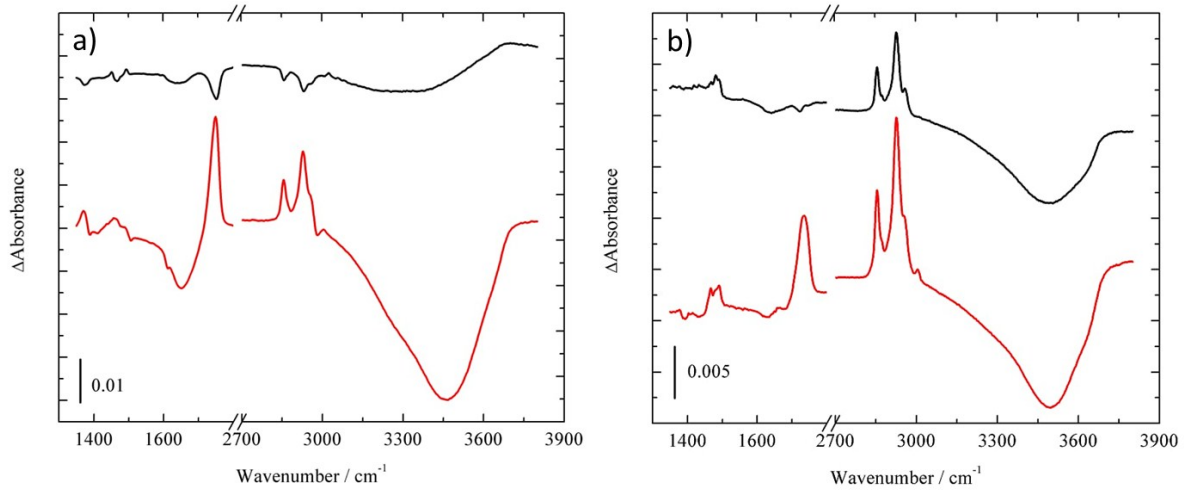

Figure S6. SEIRAS spectra recording the deposition of PS-COOH (a) and PS-NH_2 (b) onto SLB at 150 mM NaF, pH 7.5. The spectra are presented as the change in absorbance referenced to the interface before adding NPs and after the formation of DOPC bilayer (black lines). Alternatively, the spectra are shown using the single beam spectrum prior to the formation of the bilayer as the reference spectrum (red lines).

These QCM-D and SEIRAS results are consistent with the Derjaguin-Landau-Verwey-Overbeek (DLVO) theory, in which the deposition was unfavorable due to enhanced electrostatic repulsion as both PS-COOH and SLB were more negatively charged at low ionic strength (Table S1).[13, 14] In addition, there was a decrease in K_{OW} of PS-COOH at 10 mM ionic strength (from 0.89 to 0.28, Table 1 and S1). Overall, when ionic strength was decreased to 10 mM, the weaker hydrophobic interaction and greater electrostatic repulsion suppressed the deposition of PS-COOH and its associated membrane disruption.

Table S1. Physicochemical properties of nanoparticles and lipid vesicles at 10 mM NaF, pH 7.5

	D_H, nm	ζ-potentials, mV	K_{OW}
PS-COOH	56.56 ± 0.17	-54.8 ± 4.11	0.28 ± 0.02
PS-NH_2	59.64 ± 0.17	30.3 ± 1.67	0.18 ± 0.11
DOPC	42.87 ± 0.19	-21.4 ± 3.61	N/A

When the ionic strength was decreased from 150 to 10 mM NaF, PS-NH_2 became less positively charged (ζ-potential = 42.2 vs 30.3 mV, Table 1 and S1). This could potentially due to the adsorption of phosphate anions onto PS-NH_2, which counteracted the compression of electrical double layer (EDL) by increasing the negatively charged anions on the surface of NPs. In contrast with the scenario of PS-COOH, the decrease of electrolyte concentration had less effect on PS-NH_2-SLB interactions. In spite of that, both QCM-D data and SEIRAS spectra indicated slightly greater interaction at low ionic strength, with more Δf and ΔD (-4 vs -1 Hz and 1.5×10^{-6} vs 0.4×10^{-6}, respectively, Figures 1b and S4b) and spectra peak intensity shift (Figures 2b and S5b). In agreement with the DLVO theory, a electrostatically favored condition resulted in greater deposition of PS-NH_2.[13] The minor difference in the deposition extent of PS-NH_2 between the two ionic strengths highlights the importance of non-DLVO forces in regulating the interactions. As PS-NH_2 appeared to be more hydrophilic than PS-COOH, and had similar K_{OW} values at the two ionic strengths (0.18 and 0.12, Tables S1 and 1), they may be associated with the phosphatidyl lipid head groups to a similar extent. Such hydrophilic attraction may dominate the PS-NH_2-SLB interactions and be relatively more important than the DLVO interactions, hence resulting in the similar extent of deposition.

Feature/Artifact of the SEIRAS spectra

The upward feature of the SEIRAS spectra, at wavenumber > ~ 3700 cm^{-1}, appeared to be an artifact as its line shape was very broad and extended above 3900 cm^{-1} (ROI 3 in Figure 2a). Inspection of the single beam data reveals a systematic shift in the energy curve at high frequencies upon the increase in ionic strength.

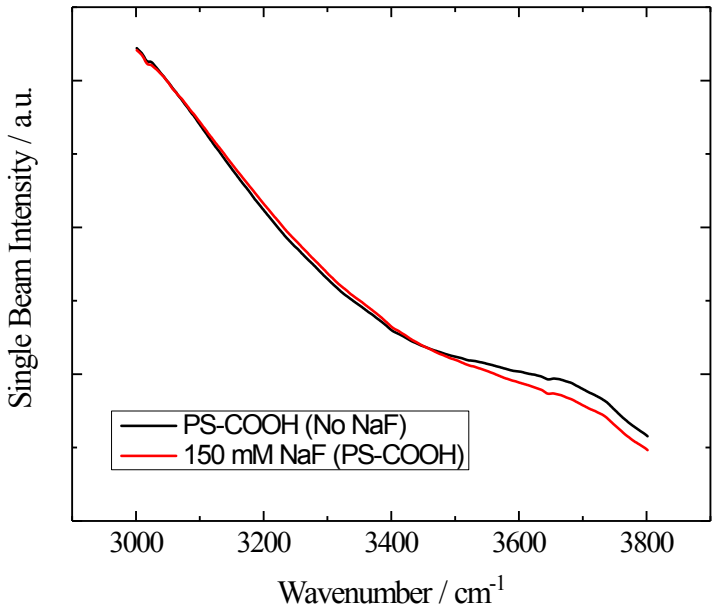

Figure S7. Single beam spectra of the PS-COOH experiment showing that the addition of the PS-COOH nanoparticles to a solution of 150 mM NaF led to a significant change in the single beam spectrum above ~ 3500 cm^{-1}

References

1. N.-J. Cho, C. W. Frank, B. Kasemo and F. Höök, Quartz crystal microbalance with dissipation monitoring of supported lipid bilayers on various substrates, *Nat. Protoc.*, 2010, **5**, 1096.
2. C. A. Keller and B. Kasemo, Surface specific kinetics of lipid vesicle adsorption measured with a quartz crystal microbalance, *Biophys. J.*, 1998, **75**, 1397-1402.
3. X. Liu and K. L. Chen, Interactions of Graphene Oxide with Model Cell Membranes: Probing Nanoparticle Attachment and Lipid Bilayer Disruption, *Langmuir*, 2015, **31**, 12076-12086.
4. X. Bin, S. L. Horswell and J. Lipkowski, Electrochemical and PM-IRRAS Studies of the Effect of Cholesterol on the Structure of a DMPC Bilayer Supported at an Au (111) Electrode Surface, Part 1: Properties of the Acyl Chains, *Biophys. J.*, 2005, **89**, 592-604.
5. S. L. Horswell, V. Zamlynny, H.-Q. Li, A. R. Merrill and J. Lipkowski, Electrochemical and PM-IRRAS studies of potential controlled transformations of phospholipid layers on Au(111) electrodes, *Faraday Discuss.*, 2002, **121**, 405-422.
6. T. Uchida, M. Osawa and J. Lipkowski, SEIRAS studies of water structure at the gold electrode surface in the presence of supported lipid bilayer, *J. Electroanal. Chem.*, 2014, **716**, 112-119.
7. A. Quirk, M. J. Lardner, Z. Tun and I. J. Burgess, Surface-Enhanced Infrared Spectroscopy and Neutron Reflectivity Studies of Ubiquinone in Hybrid Bilayer Membranes under Potential Control, *Langmuir*, 2016, **32**, 2225-2235.
8. S. R. Tabaei, J.-H. Choi, G. Haw Zan, V. P. Zhdanov and N.-J. Cho, Solvent-Assisted Lipid Bilayer Formation on Silicon Dioxide and Gold, *Langmuir*, 2014, **30**, 10363-10373.
9. S. R. Tabaei, J. A. Jackman, S.-O. Kim, V. P. Zhdanov and N.-J. Cho, Solvent-Assisted Lipid Self-Assembly at Hydrophilic Surfaces: Factors Influencing the Formation of Supported Membranes, *Langmuir*, 2015, **31**, 3125-3134.
10. I. Zawisza, A. Lachenwitzer, V. Zamlynny, S. L. Horswell, J. D. Goddard and J. Lipkowski, Electrochemical and Photon Polarization Modulation Infrared Reflection Absorption Spectroscopy Study of the Electric Field Driven Transformations of a Phospholipid Bilayer Supported at a Gold Electrode Surface, *Biophys. J.*, 2003, **85**, 4055-4075.

11. I. Zawisza, X. Bin and J. Lipkowski, Spectroelectrochemical studies of bilayers of phospholipids in gel and liquid state on Au(111) electrode surface, *Bioelectrochemistry*, 2004, **63**, 137-147.
12. K. P. Coolbear, C. B. Berde and K. M. W. Keough, Gel to liquid-crystalline phase transitions of aqueous dispersions of polyunsaturated mixed-acid phosphatidylcholines, *Biochemistry*, 1983, **22**, 1466-1473.
13. E. J. W. Verwey, Theory of the Stability of Lyophobic Colloids, *J. Phys. Colloid Chem.*, 1947, **51**, 631-636.
14. B. Derjaguin and L. Landau, Theory of the stability of strongly charged lyophobic sols and of the adhesion of strongly charged particles in solutions of electrolytes, *Prog. Surf. Sci.*, 1993, **43**, 30-59.